IAEA nuclear fusion

PAPER • OPEN ACCESS

Estimation of turbulent transport coefficients by the conditional variance method

To cite this article: T. Tork *et al* 2025 *Nucl. Fusion* **65** 016054

OPEN ACCESS
IOP Publishing | International Atomic Energy Agency
Nuclear Fusion
Nucl. Fusion 65 (2025) 016054 (5pp)
https://doi.org/10.1088/1741-4326/ad9ab7

Estimation of turbulent transport coefficients by the conditional variance method

T. Tork[1,2,*], P. Manz[2], N.H. Bian[3], F. Reimold[1], G. Grenfell[4], C. Killer[1], W. Zholobenko[4], the ASDEX Upgrade Team[a] and the W7-X Team[b]

[1] Max Planck Institute for Plasma Physics, Wendelsteinstr. 1, 17491 Greifswald, Germany
[2] Institute of Physics, University of Greifswald, 17489 Greifswald, Germany
[3] Department of Space Science, University of Alabama in Huntsville, Huntsville, AL 35899, United States of America
[4] Max Planck Institute for Plasma Physics, Boltzmannstr. 2, 85748 Garching, Germany

E-mail: tobias.tork@ipp.mpg.de

Received 19 August 2024, revised 16 November 2024
Accepted for publication 5 December 2024
Published 12 December 2024

Abstract
A novel approach for estimating turbulent transport coefficients in fusion devices is presented. The diagnostic method is established on the analysis of the conditional variance of one-point time series of density or temperature fluctuations. It is tested on data obtained from probe measurements in the edge of the tokamak ASDEX Upgrade and the stellarator Wendelstein 7-X, and on synthetic data from the gyrofluid transport model GEMR. The approach demonstrates a remarkable degree of accuracy, typically within a factor of two of the actual transport measured by more difficult means. It is a simple and accurate way of evaluating turbulent particle and heat transport coefficients that does not require measurements of the velocity fluctuations.

Keywords: turbulence, turbulent transport, diffusion coefficient, conditional moment

(Some figures may appear in colour only in the online journal)

1. Introduction

In the quest for the control of sustained thermonuclear fusion reactions, magnetic confinement of high-temperature plasma is a very attractive route. We expect from the continuing effort of technological and fundamental research that tokamaks and other magnetic confinement devices, such as stellarators, can become commercially viable sources of renewable non-fossil energy in a near future.

A major impediment to plasma confinement is turbulence. When Bohm proposed his renowned diffusion formula [1], he prophesied that 'a plasma in a magnetic field is always in a state of turbulent flow'. Turbulent fluctuations were observed in the first generation of tokamaks [2]. By the end of the last century at the latest, it became clear that turbulence is one of, if not the main obstacle to controlled nuclear fusion [3]. Turbulence affects all areas of fusion reactors, from the core [4] to the very edge [5]. It is therefore not surprising that plasma turbulence remains a subject of foremost interest [6–9]. Due to the harsh conditions inside the vessel, *in-situ* measurements of particle and heat fluxes by invasive diagnostics are challenging. They require simultaneous measurements of the velocity and of the density or temperature fluctuations in the plasma. Many magnetic confinement devices are equipped with non-invasive diagnostics such as reflectometry, beam

[a] See Zohm *et al* 2024 (https://doi.org/10.1088/1741-4326/ad249d) for the ASDEX Upgrade Team.
[b] See Grulke *et al* 2024 (https://doi.org/10.1088/1741-4326/ad2f4d) for the W7-X Team.
[*] Author to whom any correspondence should be addressed.

emission spectroscopy or Thomson scattering. They can be used to infer the density or temperature fluctuations, but not the velocity fluctuations. Such measurements are, at this time, only available using heavy ion beam probes. They constitute a very expensive diagnostic and only a few experiments have this diagnostic at their disposal.

It is the purpose of this work to present a simple and accurate method for evaluating the time-averaged turbulent flux in the direction of the gradient driving the turbulence. The method relies on density or temperature measurements but does not require measurements of the drift-velocity. From the results of numerical simulations with the GEMR code, in combination with the analysis of *in-situ* measurements in the tokamak ASDEX Upgrade (AUG) and the stellarator Wendelstein 7-X (W7-X), we investigate the conjecture that the turbulent transport can be accurately estimated from a conditional moment.

2. The conditional variance method (CVM)

The radial transport of particles across the magnetic flux surfaces can be quantified by the turbulent diffusivity

$$D_{\mathrm{T}} = -\frac{\langle \tilde{u}_{\mathrm{r}} \tilde{n} \rangle}{\nabla_{\mathrm{r}} \langle n \rangle}. \tag{1}$$

Here, $\langle . \rangle$ denotes the ensemble average, $\tilde{n}$ is the fluctuating density and $\tilde{u}_{\mathrm{r}}$ is the fluctuating radial component of the drift-velocity of the ions and the electrons in a toroidal geometry. Due to the presence of a mean radial density gradient maintained by the sources, the initial production of density fluctuation variance $\langle \tilde{n}^2 \rangle$ at a given location in space, is governed by

$$\frac{1}{2}\frac{\partial}{\partial t}\langle \tilde{n}^2 (t) \rangle = D_{\mathrm{T}} \left[\nabla_{\mathrm{r}} \langle n \rangle\right]^2, \tag{2}$$

when $\tilde{n} = 0$ initially. Equation (2) derives from a quasilinear approximation. Let us introduce the *fluctuating* mixing-length,

$$R_n (t) = -\frac{\tilde{n}(t)}{\nabla_{\mathrm{r}} \langle n \rangle}, \tag{3}$$

which satisfies $\partial \langle R_n^2(t) \rangle / \partial t = 2 D_{\mathrm{T}}$ for a given $\nabla_{\mathrm{r}} \langle n \rangle$. The important practical point here, is that measurements of $R_n(t)$ only require measurements of the density. We shall test the conjecture that the turbulent diffusivity D_{T} is accurately estimated from

$$D_{\mathrm{CV}} = \lim_{\tau \to 0} \frac{1}{2\tau} \langle [R_n (t+\tau) - R_n (t)]^2 | R_n (t) = 0 \rangle. \tag{4}$$

D_{CV} is the second-order moment of the increments $R_n(t+\tau) - R_n(t)$, *conditional* to $R_n(t) = 0$, in the limit $\tau \to 0$. We thus ask, to which extent

$$D_{\mathrm{T}} \stackrel{?}{=} D_{\mathrm{CV}}. \tag{5}$$

D_{CV} is evaluated from equation (4) using a linear fit to the data. We call the approach the CVM.

3. Motivating the CVM

The challenge in the CVM essentially consists in inferring the time-averaged turbulent flux $\Gamma_{\mathrm{r}} = \langle \tilde{u}_{\mathrm{r}} \tilde{n} \rangle$, at one spatial location, only from the statistics of the density fluctuations $\tilde{n}(t)$ and knowing the background density gradient $\nabla_{\mathrm{r}} \langle n \rangle$ at this location. The conjecture is prompted by equation (2). In a thought experiment, we reset the turbulent plasma into the hypothetical state of a negligibly small level of density fluctuations. For a given $\nabla_{\mathrm{r}} \langle n \rangle$, it follows from equation (2) that $\langle R_n^2(t) \rangle$ ought to grow linearly from $R_n(t=0) = 0$ at a rate given by D_{T}. It is the motivation for conditioning the second-order moment of the increments $R_n(t+\tau) - R_n(t)$ with respect to $R_n(t) = 0$ in order to evaluate D_{T} via equation (5). The saturation of the fluctuation variance $\langle R_n^2(t) \rangle$ to a local steady-state value $\langle R_n^2 \rangle$ generally involves a balance between the production, the spatial spread and the destruction of the variance. The precise nature of the saturation mechanisms only plays a secondary role in the approach here adopted to estimate the turbulent diffusivity D_{T} for the reason that the CVM uses $R_n(t) = 0$ as a pivot point.

The second-order conditional moment in equation (4) is in fact the second coefficient that appears in the Kramers–Moyal expansion of the master equation for the evolution of the probability density function $P(R_n, t)$: D_{CV} coincides with the diffusion coefficient $D_2(R_n)$ evaluated at $R_n = 0$ in a Fokker–Planck model for the evolution of $P(R_n, t)$ [10]. The validity of the master equation only relies on the assumption that $R_n(t)$ is a Markov process. All the coefficients entering the Kramers–Moyal expansion can in principle be determined from the measured time series of the time-dependent mixing length $R_n(t)$ by evaluating the kth order moments of $R_n(t+\tau) - R_n(t)$ conditioned to $R_n(t) = R_n$. When truncated to the two first conditional moments, such a framework forms the basis of the dynamical approach that consists in modeling the time series by a Langevin equation, akin of the scheme designed by Friedrich and Peinke for two-point turbulence data [11].

Here, we analyze one-point measurements in order to evaluate spatial transport coefficients. Therefore, the CVM does not necessarily require $R_n(t)$ to be a Markov process, neither does it require the evaluation of any other conditional moments except the second-order one. All the conditional moments, and more particularly the drift coefficient $D_1(R_n)$, are necessary for describing the evolution of $P(R_n, t)$ toward a steady-state distribution. We emphasize that the Markov property should not be confused with the absence of temporal correlations. The standard example of a Markov process with finite correlation time is given by the Ornstein–Uhlenbeck process. Up to rescaling, it is the only stationary Markov process with Gaussian statistics. Let us assume that the time-dependent mixing length $R_n(t)$ behaves as the Ornstein–Uhlenbeck process with linear drift $D_1(R_n) = \alpha R_n$ and constant diffusion coefficient $D_2(R_n) = D_2$. It follows that, starting from $R_n(t=0) = 0$ the variance increases toward a steady-state value according to $(D_2/\alpha) \times [1 - \exp(-2\alpha t)]$. In this case, it yields $D_{\mathrm{CV}} = D_2$, for the initial linear growth of the variance from a state with vanishing level of fluctuations. As a diagnostic tool, the CVM is not intended to model the time-dependent mixing length

$R_n(t)$ by any particular stochastic process, neither it attempts to predict the large time evolution of $P(R_n,t)$ toward a steady-state distribution $P(R_n)$. Nevertheless, the steady-state distribution is observed to have a Gaussian core around $R_n = 0$, in both the numerical and the experimental data that are analyzed below. It makes the Ornstein–Uhlenbeck process an eligible model for the time-dependent mixing length.

4. Validation of the CVM from numerical data

We start by testing the CVM on electron transport in simulations performed with GEMR. GEMR is a global three-dimensional electromagnetic delta-f gyrofluid model for plasma turbulence in the edge of tokamaks [12]. An important feature of the model is that it exhibits an equilibrium that is self-consistent with the turbulent transport. We run the GEMR code with AUG parameters (major radius $R = 1.65$ m, minor radius $a = 0.5$ m, magnetic field strength $B = 2.5$ T, safety factor $q_s = 4.6$) at a temperature of 60 eV and using four distinct reference plasma densities ranging from $1\times10^{19}\,\mathrm{m}^{-3}$ to $4\times10^{19}\,\mathrm{m}^{-3}$. Along with the density, the adiabaticity parameter changes and thus also the ratio between drift and interchange turbulence [13, 14]. Simulation data are collected in the outboard mid-plane at 10 different radial locations that are spaced apart by a distance larger than the radial correlation length of density fluctuations. This covers the plasma edge region from 2 cm inside to 1 cm outside the last closed flux surface, where the outside part is called the near scrape-off layer (SOL). Source and sink regions are excluded. Velocity fluctuation measurements are not possible in the near-SOL region without the risk of damaging the probes due to extreme thermal stress levels. Such measurements are more common in the far-SOL where profiles are notably flattened. There, the turbulent flux is affected by non-local transport effects [15] originating from deeper within the plasma [16, 17]. Applying the CVM to the far-SOL is expected to yield an overestimation of the transport.

The turbulent cross-field transport of particles with sub-Alfvénic speeds is primarily electrostatic in a low-β plasma. Consequently, the turbulent diffusivity is computed from the dominant electrostatic contribution via $D_\mathrm{T} = -\Gamma_\mathrm{r}/\nabla_\mathrm{r}\langle n\rangle$. Here, $\Gamma_\mathrm{r} = \langle\tilde{n}\tilde{E}_y\rangle/B$ represents the time-averaged $E\times B$ flux of particles mediated by the radial electric drift-velocity $\tilde{u}_\mathrm{r} = \tilde{E}_y/B$ and $\tilde{E}_y$ denotes the bi-normal component of the electric field fluctuations. The conditional variance D_CV is computed from the time series $R_n(t)$ according to equation (4). The turbulent diffusivity D_T and the conditional variance D_CV are compared in figure 1. The four different colors correspond to the four different reference densities, from low (dark blue) to high (red), yielding two orders of magnitude variation in the transport coefficient. Estimations of the turbulent diffusivity by the CVM (colored squares) display a remarkable degree of accuracy. D_CV does not deviate by more than twice D_T in all the simulations.

It is interesting to compare the CVM with other heuristic approaches aimed at estimating turbulent transport coefficients. In the case when there are no available measurements of the drift-velocity, a gold standard remains the mixing length model (MLM). From measurements of the radial correlation length L_C and of the correlation time τ_C of the density fluctuations, the turbulent diffusivity can be estimated from $D_\mathrm{T} = L_\mathrm{C}^2/2\tau_\mathrm{C}$ in the MLM. We emphasize that contrary to the CVM, the MLM does require simultaneous measurements of density fluctuations at different radial locations. From figure 1, we observe that the MLM severely overestimates D_T, particularly in the deep regions of higher density and temperature in the plasma where the turbulence intensity is smaller. The MLM derives from consideration of the correlation scales of the number density only, without taking into account the effects of the cross-correlation between the density and the electrostatic potential, e.g. the cross-phase in a Fourier decomposition in space. As the spatially local growth rate of density fluctuation variance $\langle\tilde{n}^2\rangle$ implicitly depends on the instantaneous value of the radial flux $\langle\tilde{u}_\mathrm{r}\tilde{n}\rangle$, the CVM is significantly more sensitive to cross-correlations, including the cross-phase, here not in the wave-number but in the frequency domain [18].

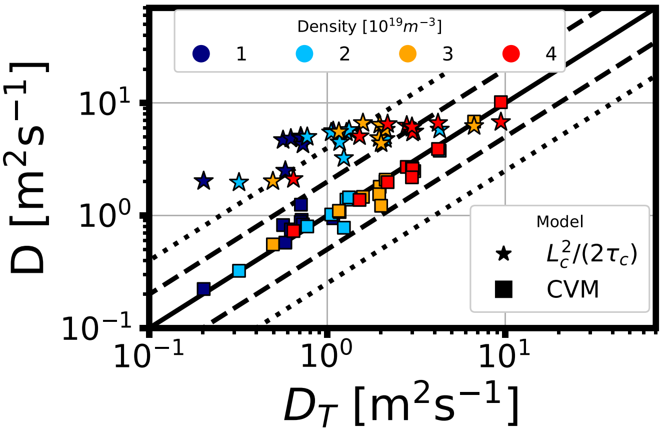

Figure 1. Evaluation of D_T using the conditional variance method and the mixing length model applied to GEMR simulation data. Colors indicate low (blue) and high (red) density runs. Stars refer to estimations made using the MLM and squares indicate those made using the CVM. Error bars are discarded for visual clarity. Dashed and dotted black lines mark deviations by a factor of two and four, respectively.

The CVM is not limited to study particle transport and it can be applied to the evaluation of turbulent heat fluxes. The turbulent heat conductivity of the electrons that is estimated from the CVM based on the fluctuating mixing length $R_{T_\mathrm{e}}(t) = -\tilde{T}_\mathrm{e}(t)/\nabla_\mathrm{r}\langle T_\mathrm{e}\rangle$ is compared to $\chi_\mathrm{T} = -\frac{2}{3}\langle\tilde{u}_\mathrm{r}\tilde{T}_\mathrm{e}\rangle/\nabla_\mathrm{r}\langle T_\mathrm{e}\rangle$ in figure 2. In terms of the degree of accuracy, the results for heat transport are similar to those obtained for particle transport.

5. Validation of the CVM from experimental data

The CVM is now tested on experimental data. In the plasma edge of fusion devices, it is possible to measure the density, the electric potential and their correlations using reciprocating probes. Since direct transport measurements are available in the edge of most fusion devices, but not in the pedestal or the core regions, the goal is here only to put the CVM to the

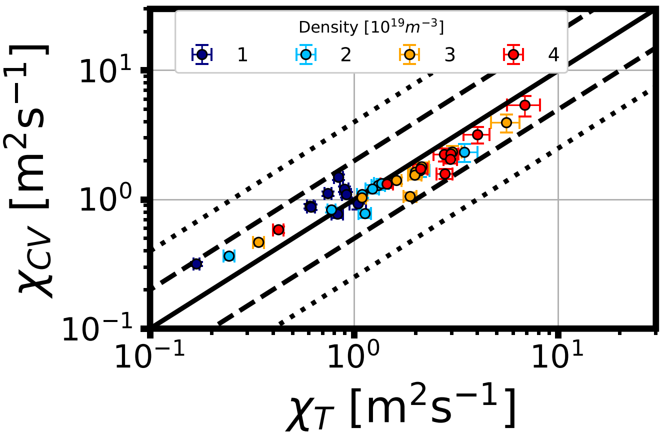

Figure 2. The CVM applied to the evaluation of the turbulent heat conductivity χ_T; the color coding is identical to figure 1.

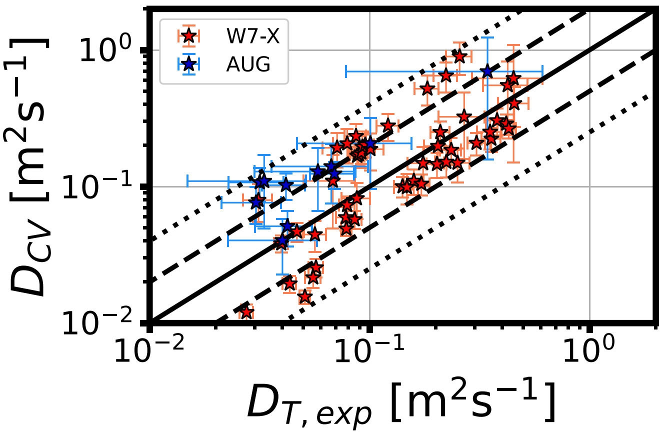

Figure 3. Comparison between $D*_T$ and D_{CV} obtained from several discharges in the stellarator W7-X (red) and the tokamak AUG (blue). The stars and the associated error bars correspond to estimations from discharges that can differ in heating power, probe penetration depth and magnetic configuration. Dashed and dotted lines mark deviations by a factor of two and four, respectively.

experimental test. An array of Langmuir and/or ball-pen probe pins is mounted on a movable manipulator that is inserted into the plasma on the outboard side. The density is derived from probe measurements of the ion saturation current. Two additional probe pins can measure the floating potential that serves as an approximation for the plasma potential. When Langmuir probes are subject to strong temperature fluctuations, the floating potential becomes a poor approximation to the plasma potential [19]. High-heat flux ball pen probes are an alternative to reduce the negative impact of the temperature on potential measurements [20]. The probe pins are arranged in such a way to allow simultaneous measurements of the density and the poloidal electric field E_θ, and hence, measurements of the radial flux $\Gamma_r \simeq \langle \tilde{n}\tilde{E}_\theta \rangle / B$. Probe movement into the plasma enables to obtain the radial density profile that is used to derive the turbulent diffusivity $D_{T,exp}$. The radial transport is estimated from measurements of the poloidal component instead of the binormal component of the electric field fluctuations that actually drives the radial $E \times B$ flux of particles. This geometrical effect introduces a small error for the turbulent diffusivity $D_{T,exp}$, which does not occur for the simulation data. The estimations by the CVM are not affected by this error. As the CVM is based on single-point measurements, finite distances between probe pins do not impact the estimations. Additionally, the approximation of the plasma potential by the floating potential has no influence on the CVM.

For the experimental validation of equation (5), probe measurements of multiple plasma discharges in W7-X and AUG are used. The W7-X data that are analyzed here, cover many different magnetic field configurations and have been published elsewhere [21]. The heating power is varied between different plasma discharges from 2 MW to 5.3 MW applied through electron cyclotron resonance heating (ECRH). An additional heating power is applied to the plasma through neutral beam injection (NBI) ranging from 0 to 3.6 MW. At the probe depth, the magnetic field is approximately 2.3 T. The plasma potential is approximated using Langmuir probes. The W7-X measurements are low-pass filtered at cutoff frequency of 50 kHz. The AUG plasma is heated by 300 kW of ECRH in addition to Ohmic heating. The magnetic field strength is 1.9 T and the plasma current is 0.8 MA in the discharges. The plasma potential is measured by ball-pen probes. A low-pass filter with a cutoff frequency of 25 kHz is applied to the data. The AUG data that are analyzed here are partially taken from [20], the remaining discharges involve deeper probe penetration. Most probe measurements are done within the plasma confinement region, some in the far-SOL.

Figure 3 shows the comparison between results of direct measurement of the transport coefficient and application of the CVM. The solid black line indicates exact agreement, the dashed (dotted) line an agreement within a factor two (four). For both W7-X and AUG data sets, the transport scaling is correctly reproduced by the CVM. A slight trend toward underestimation is observed in W7-X, while application of the CVM to AUG displays the inverse tendency despite the uncertainties being larger.

6. Summary and conclusion

In summary, the CVM is proposed as a new approach for estimating turbulent transport coefficients in fusion devices, leveraging fluctuation data and background profile gradients. The transport coefficients are determined from the spatially local growth rate of the variance of density or temperature fluctuations conditioned to small deviations from their mean. For this purpose, we use a conditional moment of the fluctuating mixing length deriving either from the density or the temperature fluctuations. Validation of the method from synthetic data yields promising results. Deviations from the actual flux of particles or energy are no larger than a factor of two while varying the transport intensity by two orders of magnitude. For experimental validation, the method is compared with direct probe measurements of particle transport in a variety of W7-X and AUG plasma discharges. While statistical scattering increases, as expected from the analysis of laboratory data, the overall scaling is well reproduced and the turbulent transport coefficients are mostly estimated within a factor of two, even considering the experimental error bars.

The major strength of the method is its applicability to the confinement region of fusion devices, where the harsh environment forbid *in-situ* measurements with invasive diagnostics. Most magnetically confined fusion experiments are equipped with diverse non-invasive diagnostics for estimating density and temperature fluctuations, as well as their profiles. The CVM is simple to apply and accurate. Given its straightforward implementation within existing diagnostic infrastructures, the CVM constitutes a powerful tool for multi-machine studies. The method is designed to investigate turbulent transport scaling with the fundamental plasma parameters of fusion devices, not only in future experimental campaigns but also from existing data.

Acknowledgments

We are grateful to Bruce Scott for providing the GEMR code. This work has been partially conducted within the framework of the EUROfusion Consortium, funded by the European Union via the Euratom Research and Training Programme (Grant Agreement No. 101052200—EUROfusion). Views and opinions expressed are those of the authors only and do not necessarily reflect those of the European Union or the European Commission. Neither the European Union nor the European Commission can be held responsible for them.

ORCID iDs

T. Tork https://orcid.org/0009-0005-1961-2431
P. Manz https://orcid.org/0000-0002-5724-0174
N.H. Bian https://orcid.org/0000-0003-0142-8669
F. Reimold https://orcid.org/0000-0003-4251-7924
G. Grenfell https://orcid.org/0000-0003-0107-5787
C. Killer https://orcid.org/0000-0001-7747-3066
W. Zholobenko https://orcid.org/0000-0002-2624-0251

References

[1] Bohm D. 1949 *The Characteristics of Electrical Discharges in Magnetic Fields* (McGraw Hill)
[2] Nedospasov A.V. 1992 Edge turbulence in tokamaks *J. Nucl. Mater.* **196–198** 90–100
[3] Horton W. 1999 Drift waves and transport *Rev. Mod. Phys.* **71** 735–78
[4] Garbet X., Idomura Y., Villard L. and Watanabe T.H. 2010 Gyrokinetic simulations of turbulent transport *Nucl. Fusion* **50** 043002
[5] Giacomin M., Pau A., Ricci P., Sauter O. and Eich T. (The ASDEX Upgrade Team, JET Contributors and The TCV Team) 2022 First-principles density limit scaling in tokamaks based on edge turbulent transport and implications for ITER *Phys. Rev. Lett.* **128** 185003
[6] Kobayashi M., Tanaka K., Ida K., Hayashi Y., Takemura Y. and Kinoshita T. 2022 Turbulence spreading into an edge stochastic magnetic layer induced by magnetic fluctuation and its impact on divertor heat load *Phys. Rev. Lett.* **128** 125001
[7] Ding S. *et al* 2024 A high-density and high-confinement tokamak plasma regime for fusion energy *Nature* **629** 1–6
[8] Xu S., Maeyama S., Watanabe T.-H. and Gürcan O.D. 2024 Reversal of the parallel drift frequency in anomalous transport of impurity ions *Phys. Rev. Lett.* **132** 105101
[9] Fasoli A. 2023 Essay: overcoming the obstacles to a magnetic fusion power plant *Phys. Rev. Lett.* **130** 220001
[10] Risken H. 1996 *The Fokker-Planck Equation: Methods of Solution and Applications* (Springer)
[11] Friedrich R. and Peinke J. 1997 Description of a turbulent cascade by a Fokker-Planck equation *Phys. Rev. Lett.* **78** 863
[12] Kendl A., Scott B.D. and Ribeiro T.T. 2010 Nonlinear gyrofluid computation of edge localized ideal ballooning modes *Phys. Plasmas* **17** 072302
[13] Scott B.D. 2005 Drift wave versus interchange turbulence in tokamak geometry: linear versus nonlinear mode structure *Phys. Plasmas* **12** 062314
[14] Eich T., Manz P., Goldston R.J., Hennequin P., David P., Faitsch M., Kurzan B., Sieglin B. and Wolfrum E. (The ASDEX Upgrade Team and The EUROfusion MST1 Team) 2020 Turbulence driven widening of the near-SOL power width in ASDEX Upgrade H-mode discharges *Nucl. Fusion* **60** 056016
[15] Manz P. *et al* 2015 Origin and turbulence spreading of plasma blobs *Phys. Plasmas* **22** 022308
[16] Boedo J.A. *et al* 2001 Transport by intermittent convection in the boundary of the DIII-D tokamak *Phys. Plasmas* **8** 4826–33
[17] Zholobenko W., Pfennig J., Stegmeir A., Body T., Ulbl P. and Jenko F. 2023 Filamentary transport in global edge-SOL simulations of ASDEX Upgrade *Nucl. Mater. Energy* **34** 101351
[18] van Milligen B.P., Carreras B.A., Voldiner I., Losada U. and Hidalgo C. (TJ-II Team) 2021 Causality, intermittence and crossphase evolution during confinement transitions in the TJ-II stellarator *Phys. Plasmas* **28** 092302
[19] Nold B., Ribeiro T.T., Ramisch M., Huang Z., Müller H.W., Scott B.D. and Stroth U. (The ASDEX Upgrade Team) 2012 Influence of temperature fluctuations on plasma turbulence investigations with Langmuir probes *New J. Phys.* **14** 063022
[20] Grenfell G. *et al* (ASDEX Upgrade Team) 2022 High-heat flux ball-pen probe head in ASDEX-Upgrade *Rev. Sci. Instrum.* **93** 023507
[21] Killer C., Narbutt Y. and Grulke O. (The W7-X Team) 2021 Turbulent transport in the scrape-off layer of Wendelstein 7-X *Nucl. Fusion* **61** 096038